Adaptive Power Pinch Analysis for Energy management of Hybrid Energy Storage Systems

Nyong-Bassey Bassey Etim[1], Damian Giaouris[1], Athanasios I. Papadopoulos[2], Haris Patsios[1], Simira Papadopoulou[2,3], Spyros Voutetakis[2], Panos Seferlis[2], Sara Walker[1], Philip Taylor[1], Shady Gadoue[4]

[1]School of Engineering, Newcastle University, Newcastle, United Kingdom

[2]Chemical Process and Energy Resources Institute, Centre for Research and Technology Hellas, 57001, Thessaloniki, Greece

[3]Department of Automation Engineering ATEI, Thessaloniki, Greece

[4]Aston University, School of Engineering and Applied Science, Birmingham, United Kingdom

B.E.Nyong-Bassey1@ncl.ac.uk

***Abstract*—This work proposes a hierarchical control based power management strategy exploiting an adaptive Power Pinch analysis algorithm. The power pinch analysis is aided via the insight-based graphical power grand composite curve (PGCC) of the hybrid energy storage system's (HESS) model. This results in the identification of an optimal power management strategy (PMS), effected at the beginning of a control horizon on the HESS. However, a recent study showed that weather and load uncertainty distorts the desired shaped PGCC and consequently leads to the violation of the energy storage's state of charge operating set points. In this work in order to negate the effect of uncertainty, the current output state is utilized as a feedback control. The PGCC is shaped within a receding horizon model predictive control framework. The PGCC re-computation ensues only if the error variance, due to uncertainty, between the real and the estimated battery's state of charge ($SOAcc_{BAT}$) is greater than 5%. The proposed method is evaluated against the standard or Day-Ahead pinch analysis open loop strategy and shows a reduction in over discharging and overcharging of the battery and fossil fuel emission impact by 15%, 44.97%, and 8.8% respectively.**

Keywords—Adaptive PMS, Adaptive Power Pinch, Power Grand composite curve, Smart Grid, MPC

I. INTRODUCTION

Renewable energy (RE) resources have seen an increase in penetration mostly due to rising concerns over the impact of greenhouse gas emission on the environment [1]. The solar energy harnessed by means of photovoltaic panels is a very favourable RE option. However, the output power fluctuates due to weather intermittency such as cloudy days as well unavailability at night. Therefore, solar energy is often integrated with energy storage systems such as batteries, supercapacitors, hydrogen energy storage etc. [2, 3]. In addition, the hybrid renewable energy systems (HRES) is a combination of one renewable energy source and one conventional energy source, or multiple renewable with or without conventional energy sources, which may be isolated or grid connected [4]. The incorporation of multiple energy storage systems for reliable power generation in a smart micro-grid, forms the concept of hybrid energy storage systems (HESS) [3]. The interaction between the HESS assets accordingly requires a power management strategy (PMS) for switching and power supply decision making in order to ensure optimal operation and prolonged life of the assets [5]. Hence, developing a reliable PMS for the HESS has become an active research topic. This brings forth the Power pinch analysis (PoPA), an insight-based graphical and algebraic process integration tool adapted from heat exchanger network pinch analysis, originally proposed by Linnhoff and Flower [6]. The PoPA has been utilized in short-term planning of power supply and demand utilization, aided by the composite curve [7]. In the power composite curve (PCC) a graphical plot of the supply and demand power curve with time is used to determine the minimum/maximum electricity pinch utility targets. In addition, load shifting via identification of peak demand to off-peak period, was employed using PoPA in [8]. Furthermore, in [9] the PoPA concept was combined within a model predictive control (MPC) framework for the first time to infer and effect energy management decisions in a hybrid stand-alone micro-grid. Additionally, the PoPA was aided using the Day-ahead power profile of the system to form the grand composite curve (GCC). The study showed that the unaccounted variation caused by seasonal variation forecasts error leads to the violation of the pinch operating points [9 - 11]. The work in this paper, proposes an adaptive PoPA based on a receding horizon MPC framework for energy management of the HESS in a bid to negate the undesired effects of forecast errors.

II. MODELLING OF HYBRID RENEWABLE ENERGY SYSTEM

As a case study, the configuration of the HRES comprises a battery (BAT), photovoltaic panels (PV), fuel cell (FC), electrolyzer (EL), water tank (WT), hydrogen tank (HT), diesel generator (DSL) and consumer load (LD). The model parameters for the HRES including PMS constraints for the HESS utilized in this work are the same as [12] for consistency.

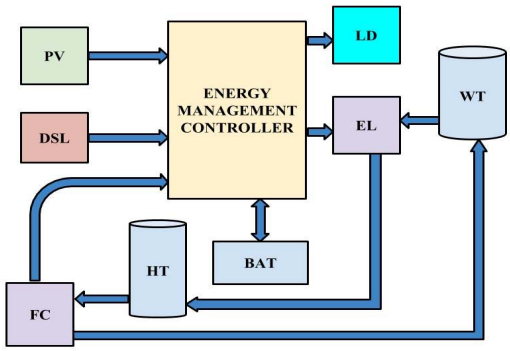

Fig. 1 HRES configuration

The interconnection of the components of the system is such that the flow of energy and matter is modelled based on the state of the energy storages, utilizing net energy graph theory concept [12]. The dynamics of the system at any instant are described as a function of the energy storages and the converters by means of the net energy.

The state of energy or material in an accumulator of capacity C_l depends on the net flow $\mathrm{F}^{j}_{x\leftrightarrow y}(\mathrm{t})$, presented as follows:

$$SOAcc_l^{n,m}(t) = SOAcc_l(t-1) + \left[\sum_{x1\in Rs^{Conv}} F^j_{l\leftarrow x1}(t) - \sum_{x2\in Rs^{Conv}} F^j_{l\rightarrow x2}(t)\right]\frac{\Delta t}{C_l} \quad (1)$$

The flow of electrical energy or material is defined as follows:

$$\mathrm{F}^{j}_{x\leftrightarrow y}(\mathrm{t}) = \varepsilon_i(\mathrm{t})\,\delta Q_i^j(t), \quad i \in \{x, y\} \quad (2)$$

Where, $\varepsilon_i(\mathrm{t})$ is a binary variable of the converter's state, δ is used for varying the magnitude of energy or material $Q_i^j(t)$ converted by the i^{th} unit. In addition, the existence of an edge, represented by the binary variable $\varepsilon_i(\mathrm{t}) \in [0,1]$, is inferred from the state of the storages $SOAcc(\mathrm{t})$ and subscript l refers to storage system. And m, n superscripts refer to the actual and estimated value of the HESS.

$$\varepsilon_i(\mathrm{t}) = L(\varepsilon_i^{Avl}(\mathrm{t}), \varepsilon_i^{Req}(\mathrm{t}), \varepsilon_i^{Gen}(\mathrm{t})) \quad (3)$$

III OVERVIEW OF THE POWER PINCH ANALYSIS CONCEPT

The main principles of the PoPA concept, as applied in power generation systems, are illustrated in Figure 2. An accumulator (e.g. hydrogen tank) stores excess energy from a converter (e.g. PV) due to saturation of another converter (e.g. battery's state of charge $SOAcc_{BAT}$>Up). Similarly, another converter (e.g. Fuel cell) utilises the stored hydrogen to maintain the $SOAcc_{BAT}$ from falling below a lower limit ($SOAcc_{BAT}$ <*Lo*). When maintenance of the system within these limits becomes impossible, they are violated. This is all shown through a plot of $SOAcc_{BAT}$ with respect to time (continuous black line in Figure 2) which is called the Power Grand Composite Curve (PGCC) of the system. In the case of the *Lo* limit, the PGCC indicates the amount of outsourced electricity required (e.g. through non-renewable resources) in order to move and keep the curve above it. In the case of the *Up* limit, the PGCC indicates the amount of energy that needs to be dumped, which is also undesirable. By shifting the entire PGCC up or down (red dot-dashed line in Figure 2), the point in time where the PGCC touches the *Lo* or *Up* lines is called the Pinch point. The new, shifted curve indicates the energy storage targets at each instant in order to operate within the desired limits. The shifted curve can be approached by initiation or termination of the appropriate converters in order to generate an overall PMS that best matches the shifted curve. Furthermore, the duty cycle of the energy storage is preserved by matching the available energy for the next day (AEEND) to be equal to the energy at start of the shifted PGCC. However, realising the PoPA successfully via Day-ahead (DA) strategy requires accurate load and weather data which is often not the case due to uncertainty. The effect the uncertainty causes a mismatch between the actual and predicted $SOAcc_{BAT}$ parameters as shown in Figure 3. Therefore violation of the upper and lower pinch may occur.

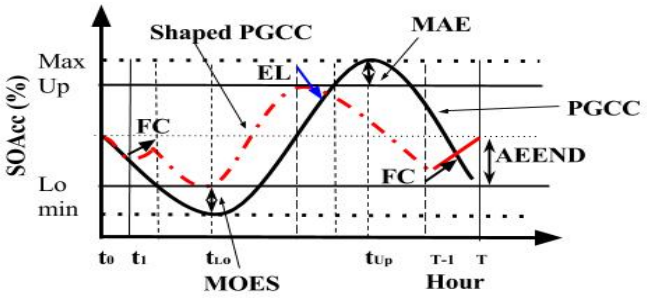

Fig. 2: PGCC shaping utilizing DA-PoPA without uncertainty

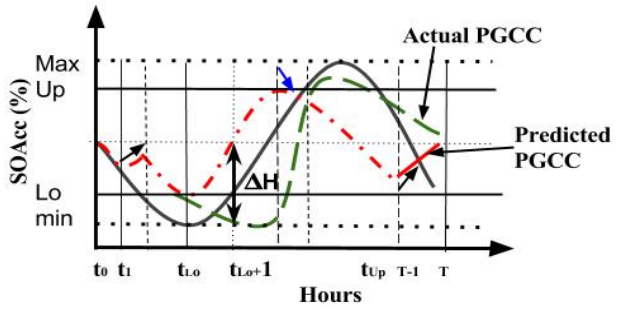

Fig 3: PGCC shaping utilizing DA-PoPA with load and weather uncertainty

IV ADAPTIVE RECEDING HORIZON POWER PINCH ANALYSIS

In this work, the PoPA concept is presented in an adaptive receding horizon model predictive control framework. The PMS which infers the appropriate energy targeting that keeps the system within limits is determined in a stepwise procedure in advance while satisfying the operational constraints, as follows;

$$J\left(SOAcc_l^n(k+1)\right) = \min_{U_c} \sum_{k=1}^{T-1} f(\varepsilon_i(k), SOAcc_l^n(k), U_c(k)) \quad (4)$$

$$S_{Lo}^l \le SOAcc_l^m(k) \le S_{Up}^l \quad (5)$$

$$SOAcc_l^n(k_0) \cong SOAcc_l^m(T-1) \quad (6)$$

$$\varepsilon_{FC}^{Gen}(k) + \varepsilon_{EL}^{Gen}(k) \le 1 \quad (7)$$

Where, S_{Lo}^l and S_{Up}^l are the lower and upper operational limits of the Battery's state of charge. $U_c(k)$ is the determined PMS resulting from PoPA minimum energy targeting which controls the flow of power and activation of the FC and EL.

The constraints imposed by (5) ensures the pinch utility set points are not violated. The duty cycle of the energy storage is preserved by the terminal constraint (6) which infers the available energy at the end of the horizon T (AEEND). The binary variable constraint (7) prevents simultaneous activation of converters that simultaneously consume and produce the same energy carrier (e.g. FC and EL).

The insight-based PGCC concept is thus utilised in resolving the minimum energy recovery targeting problem, algebraically in two stages [8]. Firstly, at t_0 the minimum outsourced energy supply (MOES) is identified by the lower Pinch utility targeting and matched with energy supplied by the FC. Secondly, the minimum absorbed energy (MAE) is targeted as well by absorbing the excess energy via the electrolyser as shown in Figure 2. Hence, the lower and upper constraints are satisfied successively to infer the desired PoPA control sequence $U_c(SOAcc_l^m)$ for *FC* or *EL* activation. The identified

PMS at the beginning of the horizon, necessitates the activation of the FC or EL respectively in order to shape the PGCC.

$$\underset{\rightarrow}{U_c}(SOAcc_l^n) := [U_k(S_{k+1}), \dots U_{T-1}(S_T), |S_{k+1:\, k\in[0,1,2,\dots,T]}]$$

The PGCC targeting is utilised iteratively so as to achieve robustness to compensate for discrepancies between the real and the estimated weather/load profile. The receding horizon model predictive control (RHMPC) PoPA, therefore, employs a state feedback loop to adapt the model to the HRES. Thus a closed loop is utilised and the estimated and real states are compared for discrepancy after each iteration so as to achieve robustness to compensate for the weather/load uncertainty. Figures 4 and 5 illustrate the adaptive receding RHMPC-PoPA algorithm and concept respectively. As shown previously in Figure 3, the degree of the PGCC violating the lower pinch utility is minimised by activating the FC after PGCC re-computation as shown by the continuous yellow line in Figure 5. Hence, minimising the effect of uncertainty ΔH between the real and the estimated state of charge is shown in equation (8).

$$\Delta\mathcal{H}(k|k) = |\mathcal{Y}^m(k) - \mathcal{Y}^n(k|k-1)| \qquad (8)$$

Where $\mathcal{Y}(k)$ is the output state measured at time *k*.

Furthermore, if $\Delta\mathcal{H}$ is greater than threshold ξ at any sampling instance, the PoPA is repeated in the predictive horizon in order to determine the optimal control sequence from that instant up until time T. The threshold error ξ is set at 5% to reduce the computational cost. The state of charge of the battery in the model for PGCC re-computation is updated as follows:

$$If\ \exists\, \Delta\mathcal{H}(k) > \xi\ , \forall_k\ , \mathcal{Y}^m(k) := f(\mathcal{Y}^n(k|k-1)) \qquad (9)$$

$$SOAcc_{BAT}^m(k|k) = SOAcc_{BAT}^m(K|K-1) \pm \Delta\mathcal{H}(k) \qquad (10)$$

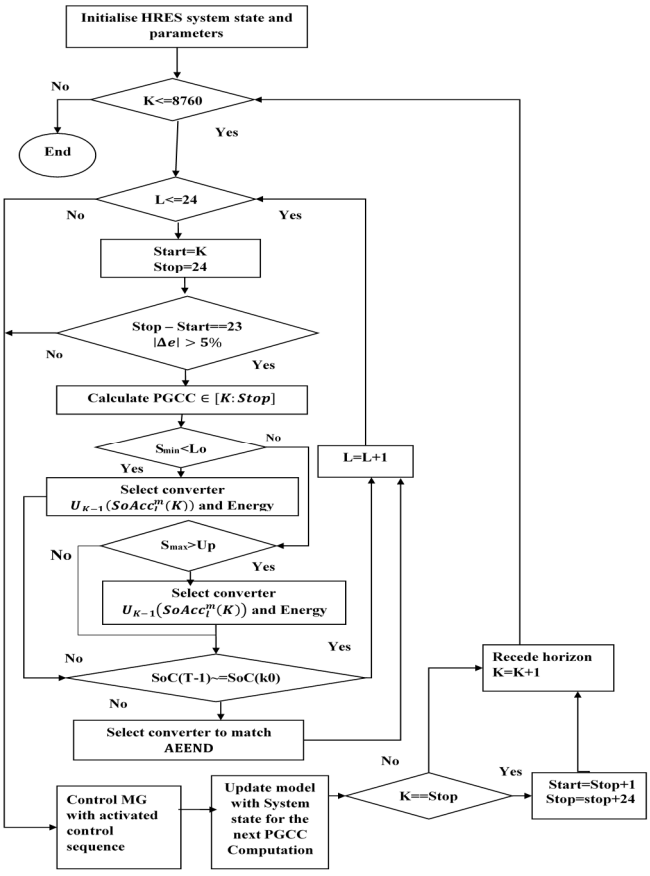

Fig 4. Adaptive RHMPC-PoPA Algorithm

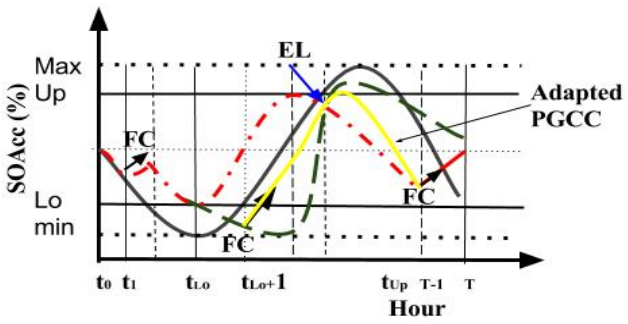

Fig 5. Re-shaped PGCC after distortion due to uncertainty

V. RESULT AND DISCUSSION

The DA-PoPA and RHMPC-PoPA PMSs are evaluated with a backup DSL power supply rated 1.3 times the maximum uncertain peak load power (1.5 KW). The DSL is only activated if the state of charge of the battery ($SOAcc_{BAT}$) is < 20%. The goal of the PMS is to ensure the $SOAcc_{BAT}$ remains between 30% and 90% during operation. The actual PV and domestic load profiles as shown in Figures 6 and 7 are derived from NREL [13] and Elexon [14] respectively.

The PV irradiance corresponds to 54.9783° N, 1.6178° W. The forecast profiles are derived by the addition of Gaussian noise $\mathcal{N}(0, 100)$ and $\mathcal{N}(0, 20)$ respectively. Table I shows the long term operation of the HRES using both PMS's.

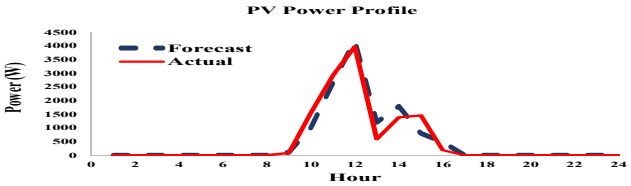

Fig. 6 PV power profile

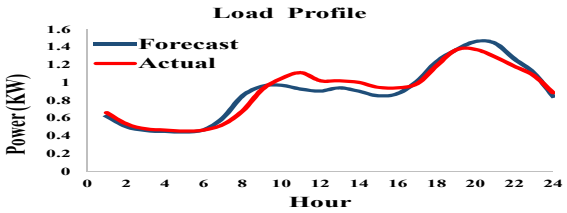

Fig. 7 Load profile

The HESS response as a result of the DA-PoPA is shown over the first 72hrs period leads to the activation of the fuel cell at the 23rd, 47th, 49th and 71st hr. The FC logic is activated to supply 8.58KWh for the AEEND at the 23rd hr. However, due to forecast error, the AEEND does not match $SOAcc_{BAT}$ corresponding to the beginning of the horizon as shown in Figure 8. Furthermore, a total of 8 violations of the lower utility occur; with 5 violations occurring between 55th and 59th hr. as well as 3 more violations between the 69th hr. to 71st hrs. These violations are due to the effect of uncertainty which was not accounted for at the beginning of the horizon. The diesel generator is activated at the 59th hr. as $SOAcc_{BAT}$ dips to 19.1% hence, violating the 20% DSL activation threshold. The DSL is turned off only at the end of the 60th hr. as seen in Figure 9 due to the hysteresis logic which maintains the DSL state until battery's $SOAcc_{BAT}$ is greater than or equal to 30%. Hence, the total power utilized from the DSL over the 72 hours period is 4.02 KW. Figure 10 shows the hydrogen and water utilization.

The RHMPC-PoPA is used to shape the original PGCC resulting in a predicted PGCC as illustrated in Figure 10a and 11b respectively. The lower utility violation which occurred using the DA-PoPA PMS is thus negated as the predicted PGCC adapts to the forecast error as seen in Figure 11c. The usage of the FC to match the AEEND at 23rd hr. as seen in Figure 12 consequently depletes the hydrogen storage at the 47th hr. while producing water. Figure 13, shows the activation of the FC logic.

From the long-term operational indices over a period of one year as presented in Table I, -the FC despite being requested for 2229 times by the RHMPC-PoPA, it is only activated 131 times due to unavailability of hydrogen. Evidently, the more frequent utilization of the FC compared to the DA-PoPA results in improved reliability but depletes hydrogen. Hence the AEEND constraint is adjusted to 50% of the $SOAcc_{BAT}$ for the analysis. Furthermore, the lower pinch is violated 1665 times out of which the $SOAcc_{BAT}$ of the battery entered the critical zone (20%<$SOAcc_{BAT}$<30%) 1423 times.

TABLE I. Performance indices for 8760 hrs operation

Operational Parameter	**PMS**	
	DA-PoPA	***RHMPC-PoPA***
FC attempt (cycles/year)	289	2229
FC start-stop (cycles/year)	61	131
EL attempts (cycles/year)	223	1017
ELstart-stop (cycles/year)	223	862
PV start-stop (cycles/year)	8084	8388
DSL start-stop (cycles/year)	894	815
Lower Pinch violation (counts/year)	1960	1665
Lower Pinch violation (counts/year) 20%<$SOAcc_{BAT}$<30%	1672	1423
Upper Pinch violation (counts/year)	676	372
Upper Pinch violation (counts/year) 90%<$SOAcc_{BAT}$<100%	568	264

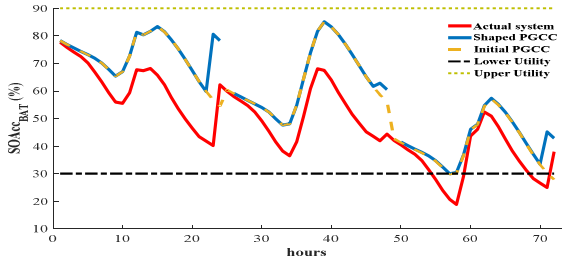

Fig. 8 The PGCC utilizing DA-PoPA

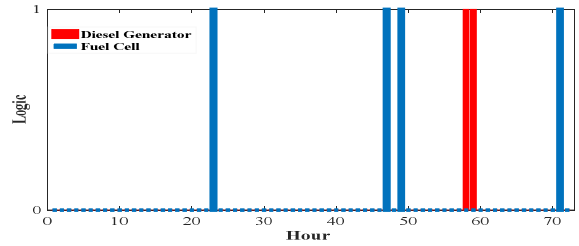

Fig. 9: DA-PoPA Converter activation logic

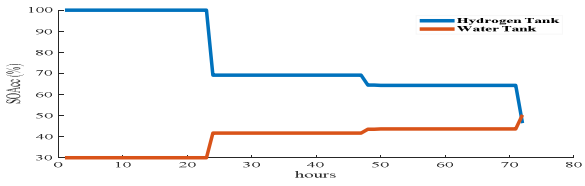

Fig. 10: DA-PoPA tank level

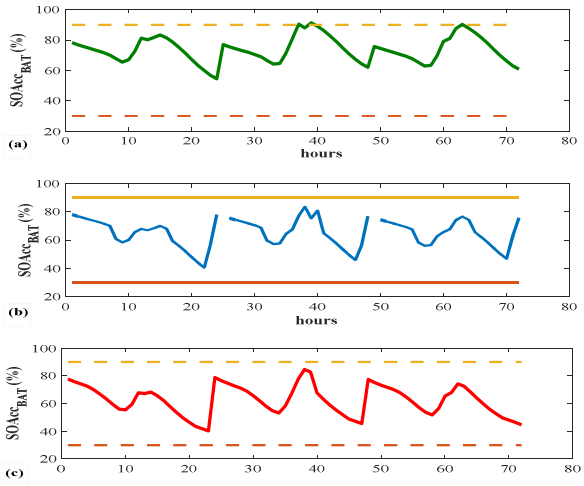

Fig. 11 a) The original PGCC based on the model of the HRES, b) the shaped PGCC in the prediction horizon and, c) the response of the HRES.

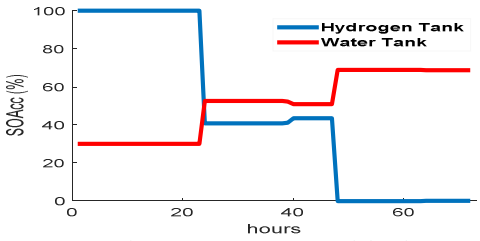

Fig. 12: RHMPC-PoPA tank level

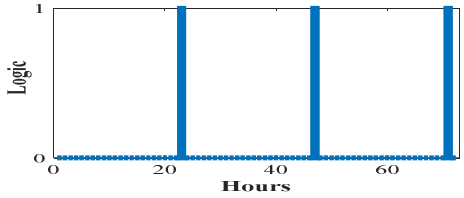

Fig 13. Converter Logic for RHMPC-PoPA

While the DA-PoPA violates the critical zone 1672 times with total lower pinch violation of 1960, this is reduced by 14.89 % and 15% respectively with the RHMPC-PoPA PMS. The increased violation of the lower utility by the DA-PoPA consequently results in the DSL being activated more frequently, 894 times. Additionally, the DA-PoPA has a 44.97% increase in the upper constraint violation with respect to the RHMPC-PoPA. Thus, the adaptive RHMPC-PoPA shows superiority over the DA-PoPA with regards to the Pinch constraint preservation.

VI. CONCLUSION

The exploitation of the PoPA in a receding adaptive model predictive (RHMPC-PoPA) framework has been presented. The RHMPC-PoPA has been evaluated against the DA-PoPA approach. In the short term utilization of both methods on a HESS, the RHMPC-PoPA shows better performance over the DA-PoPA as no utility violation occurred due to the adaptive feature via the model error correction mechanism. Furthermore, in the long term operation, the RHMPC-PoPA PMS results in a more frequent activation of the HESS assets, a trade-off for reliability. However, over-discharging, over-charging of the battery and fossil fuel emission impacts were reduced by 15%, 44.97%, 8.8% respectively, compared with the DA-PoPA PMS.

REFERENCES

[1] W. S. Ho, C. S. Khor, H. Hashim, S. Macchietto, and J. J. Klemeš, "Sahppa: a novel power pinch analysis approach for the design of off-grid hybrid energy systems," Clean Technologies and Environmental Policy, vol. 16, no. 5, pp. 957–970, Jun 2014.

[2] T. Alnejailli, S. Drid, D. Mehdi, L. C. Alaoui, R. Belarbi, and A. Hamdouni, "Dynamic control and advance load management of a stand-alone hybrid renewable power system for remote housing," Energy Convers. Manage., vol. 105, pp. 377–392, 2015.

[3] W. Jing, C. Hung Lai, S. H. W. Wong, M. L. D. Wong, "Battery-supercapacitor hybrid energy storage system in standalone DC microgrids: areview", IET Renewable Power Generation, vol. 11, no. 4, pp. 461-469, 2017.

[4] P. Bajpai, V. Dash, "Hybrid renewable energy systems for power generation in stand-alone applications: A review", Renew. Sustain. Energy Rev., vol. 16, no. 5, pp. 2926-2939, Jun. 2012.

[5] A. Brka, Y. M. Al-Abdeli, and G. Kothapalli, "Predictive power management strategies for stand-alone hydrogen systems: Operational impact," International Journal of Hydrogen Energy, vol. 41, no. 16, pp. 6685 – 6698, 2016.

[6] D. Giaouris, A. I. Papadopoulos, S. Voutetakis, S. Papadopoulou, and P. Seferlis, "A power grand composite curves approach for analysis and adaptive operation of renewable energy smart grids," Clean Technologies and Environmental Policy, vol. 17, no. 5, pp. 1171–1193, Jun 2015.

[7] S. R. W. Alwi, N. E. M. Rozali, Z. Abdul-Manan, and J. J. KlemeÅ¡, "A process integration targeting method for hybrid power systems," Energy, vol. 44, no. 1, pp. 6 – 10, 2012, integration and Energy System Engineering, European Symposium on Computer-Aided Process Engineering 2011.

[8] N. E. M. Rozali, S. R. W. Alwi, Z. A. Manan, J. J. KlemeÅ¡, and M. Y. Hassan, "Cost-effective load shifting for hybrid power systems using power pinch analysis," Energy Procedia, vol. 61, pp. 2464 – 2468, 2014, international Conference on Applied Energy, ICAE2014.

[9] D. Giaouris, A. I. Papadopoulos, P. Seferlis, S. Voutetakis, and S. Papadopoulou, "Power grand composite curves shaping for adaptive energy management of hybrid microgrids," Renewable Energy, vol. 95, pp. 433 – 448, 2016.

[10] N. E. M. Rozali and M. S. M. Yahaya, "Study of the effects of seasonal climate variations on hybrid power systems using power pinch analysis," Procedia Engineering, vol. 148, pp. 1030 – 1033, 2016, proceeding of 4th International Conference on Process Engineering and Advanced Materials (ICPEAM 2016).

[11] S. Bandyopadhyay, "Design of renewable energy systems incorporating uncertainties through pinch analysis," in 21st European Symposium on Computer Aided Process Engineering, ser. Computer Aided Chemical Engineering, E. Pistikopoulos, M. Georgiadis, and A. Kokossis, Eds. Elsevier, 2011, vol. 29, pp. 1994 – 1998.

[12] D. Giaouris, A. I. Papadopoulos, C. Ziogou, D. Ipsakis, S. Voutetakis, S. Papadopoulou, P. Seferlis, F. Stergiopoulos, and C. Elmasides, "Performance investigation of a hybrid renewable power generation and storage system using systemic power management models," Energy, vol. 61, pp. 621 – 635, 2013.

[13] Available at: http://pvwatts.nrel.gov/pvwatts.php [Accessed 1st Nov 2017].

[14] Available at: http://data.ukedc.rl.ac.uk/simplebrowse/edc/efficiency/residential/LoadProfile/data [Accessed 1 Nov. 2017]